

## Theoretical investigation of estimation of steady and pulsatile blood flow and blood vessel cross section by CW NMR excitation†

Dilip Kumar De

Department of Radiology, Bowman Gray School of Medicine, 300 S. Hawthorne Road, Winston-Salem, NC 27103, USA

Received 12 July 1988, in final form 15 August 1989

**Abstract.** In this paper we show theoretically that when a magnetised blood bolus enters a CW NMR excitor coil of length  $L_e$  at resonance and the signal from the  $T_2$ -decaying, precessing transverse magnetisation of the flowing blood spins is subsequently detected by a detector coil of length  $L$  separated from the excitor coil by a distance  $\Delta l$ , then by recording CW NMR signals at three positions such as  $\Delta l = 0, 0.5$  and  $1.0$  cm one can eliminate the static tissue signal and measure non-invasively the steady component  $V_0$  as well as the total vessel cross section,  $\beta$  accurately. The time dependent part of the CW NMR signal which depends on  $V_{\text{pulse}}(t)$ , is also dependent on  $V_0$  non-linearly unless both  $L$  and  $L_e$  are greater than 50 cm and  $\Delta l$  is zero. Finally, methods of obtaining true  $V_{\text{pulse}}(t)$  from the CW NMR signal after applying proper correction due to the steady flow are discussed.

### 1. Introduction

Knowledge of blood flow velocity or volume flow rate through the vessels of various organs of the body is important for a number of clinical applications (Caro *et al* 1978). An accurate measurement of blood velocity as a function of time has value as an indicator of heart and vessel disease. Similarly, a profile of the distribution of the blood velocity across the vessels indicates the presence or absence of obstructions in the vessels.

Nuclear magnetic resonance (NMR) offers two methods of measuring blood flow: (1) pulse NMR and (2) CW NMR excitation. Pulse NMR is further divided into the *pulse imaging method* (Battocletti *et al* 1981, Moran 1982, Axel 1984, Van Dijk 1984, Redpath *et al* 1984, O'Donnell 1985, Axel *et al* 1986, Moran *et al* 1987, Saloner *et al* 1987) and the *pulse flow method* (Singer 1959, Stejskal and Tanner 1965, Hayward *et al* 1972, Singer and Grover 1972, Heminaga *et al* 1977, Battocletti *et al* 1979). In the pulse flow method, it is difficult to correlate the detected signal strength with the flow rates because of the presence of magnetic field inhomogeneities. A field inhomogeneity of the order of only 0.8 mG, i.e. less than 1 ppm, can completely dephase the blood spins with  $T_2 = 0.15$  s. These inhomogeneities tend to dephase the excited spins before they can reach the detector. In this case, the NMR signal strength in the detector coil, is a complicated function of RF pulse width, flow velocities and effective  $T_2$ . Although experiments using a single NMR detector/receiver coil have shown correlation between

† This paper was presented at the Radiological Society of North America 74th Scientific Assembly, Annual Meeting in Chicago on 28 November 1988.

the changes in measured effective relaxation time  $T_2$  and flow (Battocletti *et al* 1979), there has not been a good theoretical description of the effects of pulsatile and steady flow components and the RF pulse width upon the detected signal. It is, however, useful to determine the steady flow velocity although flow rates cannot be measured. A recent theoretical study (Devine *et al* 1982) attempted to correlate the steady flow component alone with the detected signal, using a separate detector coil in pulse NMR. Because the effective  $T_2$  depends sensitively on the magnetic field  $B_0$  inhomogeneity, which is difficult to measure precisely, results of such attempts are not reliable. These methods would require a field homogeneity higher than 0.8 mG. For  $B_0$  of the order of 1 T, homogeneity of the order of 8 parts in  $10^8$  would be necessary.

CW NMR has an advantage over pulse flow NMR in that the field inhomogeneity (FI) is not critical to the accuracy of the CW method. If the maximum FI remains less than the RF  $B_1$  field, CW NMR yields reliable results. There has been significant interest in the real-time quantitative estimation of blood flow by CW NMR. Several papers report the application of the CW NMR technique to the estimation of blood flow using both flat and cylindrical crossed coil detectors and excitors (Halbach *et al* 1980, Salles-Cunha *et al* 1981, 1982, Battocletti 1986). In a CW system that uses a detector coil overlapping the excitor coil (or a single excitor/detector coil), estimation of steady blood flow is impeded by the overwhelming influence of static tissue signal on the time-independent steady flow signal. Such systems cannot separate the contribution of the signal ( $I_s$ ) due to the flowing blood spins from the signal ( $I_{st}$ ) due to the static tissues. Because most of the detection system is based on the  $T_2$ -decay of the precessing transverse magnetisation, the decay is exponential and, therefore, a non-linear function of velocity. The estimation of the pulsatile flow component from the measured peak-to-peak signal is therefore erroneous without correction relative to the steady flow component when a detector coil of finite size is used. The present investigation shows that the steady flow affects the time-dependent part of the NMR signal significantly, unless large excitor and detector coils are used contiguous with one another (i.e.  $L_e, L > 50$  cm, and  $\Delta l = 0$  in figure 1).

This paper presents a model, CW NMR method, an analysis of signal dependence on flow velocity, vessel cross section,  $T_2$  relaxation rates of blood spins and physical parameters of the CW system. A discussion of methods for obtaining steady velocity  $V_0$  and flow rate  $Q$  by eliminating the static tissue signal for both plug and parabolic flow by a CW NMR method has been made. In addition, extraction of accurate pulsatile flow rates after adjusting for the steady flow components is also discussed.

## 2. Theory

The simple geometrical arrangement of the CW NMR system under consideration is shown in figure 1. CW NMR excitation is carried out over the excitor coil of length  $L_e = X_2 - X_1$ . A fluid flowing in from the left is assumed to be magnetised to an equilibrium value  $M_0$  before entering the excitor coil (figure 1). Static tissue in the excitor coil region is also subjected to CW excitation. The  $B_0$  field inhomogeneity should be less than that of the RF  $B_1$  field of the RF excitation. The theoretical analysis of the dependence of NMR signal on flow rates begins with a model system in which  $B_1$  is zero outside the excitor coil. Finite  $B_1$  outside the excitor coil does not alter the conclusions reached with the model system. Beyond the excitation coil length, a detector coil receives the signal from the blood excited in the excitor coil region; the detector coil can be positioned at different distances  $\Delta l$  from the excitor coil. The

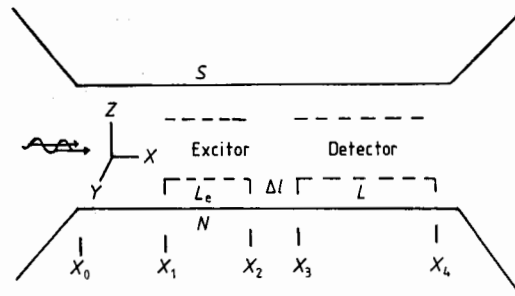


**Figure 1.** Diagram of the new CW NMR excitation scheme with separate movable detection system for accurate estimation of  $V_0$ ,  $V_{\text{pulse}}^0$  and also total cross section of the blood vessel.  $L_e$  is the length of the excitor coil.  $\Delta l$  is the separation of the excitor coil and the detector coil whose length is  $L$ .

signal is the result of the precessing transverse magnetisation,  $M_y$ , of the flowing spins and is dependent on both the flow velocity and on the  $T_2$  relaxation time.

In the following,  $\gamma$  denotes the gyromagnetic ratio of blood spins;  $\omega/2\pi$  is the RF excitation frequency;  $f_0/\gamma$  is the off-resonance field in the rotating frame of reference. The detector coil should be in the cross coil mode of detection, i.e. orthogonal to the excitor coil. To further reduce the direct feedthrough from the excitor, the RF excitation is modulated by about 5-8 KHz, and the detection is tuned to one of the side bands instead of the main resonance. By using proper shielding, the direct coupling between the excitor and detector coils can be further minimised. The detector, being separated from the excitor, would receive only a very small amount of static tissue signal.

In figure 1 we assume  $f_0 = 0$  (i.e. at resonance condition within the entire excitor coil) where  $f_0 = \gamma B_0 - \omega$  and  $\gamma$  is the gyromagnetic ratio of blood spin;  $\omega/2\pi$  is the RF excitation frequency;  $f_0/\gamma$  is the off-resonance field in the rotating frame. The  $x$ ,  $y$ ,  $z$  components of magnetisation are given by the Bloch equations (Slichter 1963), which may be written as follows

$$dM_x/dt = -M_x/T_2 \quad (1a)$$

$$dM_y/dt = \gamma[M_z B_1(X)] - M_y/T_2 \quad (1b)$$

$$dM_z/dt = -\gamma M_y B_1 + (M_0 - M_z)/T_1 \quad (1c)$$

where  $x$ ,  $y$ ,  $z$  axes are of the rotating frame of reference. The  $z$  axis is along the laboratory  $Z$  axis, whereas the  $x$  and  $y$  axes form an angle  $\omega t$  with the laboratory  $X$  and  $Y$  axes, respectively.

$M_z$  of the blood within the excitor coil differs from  $M_0$  on the order of  $B_1^2$ . Thus, if  $B_1$  is small,  $M_z = M_0$  in the first approximation. From these equations,

$$M_+ = A \exp(-at) + i\gamma M_0 B_1 / (1/T_2 + if_0) \quad (1d)$$

$$M_+ = M_x + iM_y$$

where

$$f_0 = \gamma B_0 - \omega, \quad M_z = M_0, \quad (1e)$$

$$a = 1/T_2 + if_0.$$

The constant  $A$  is defined in equation (3a).

The first term in equation (1d) is negligible for static tissues. However, this term cannot be ignored for a bolus of steady blood flow or a pulsatile blood flow. For a

given blood bolus flowing with steady velocity  $V_0$ , time  $t=0$  is the moment the given bolus enters the excitation region at  $X_1$  (i.e.  $t = X/V_0$ ,  $X$  is the distance traversed by the blood bolus as measured from  $X_1$  (figure 1)).

### 2.1. Steady blood flow

For blood flowing with steady velocity  $V_0$ , the  $M_x$  and  $M_y$  components can be separated from  $M_+$  in equations (1d) and (1e). For a given blood bolus at any position  $X$  measured from  $X_1$  ( $X_1 < X < X_2$ ),

$$M_x = A(1 - \exp(-X/(V_0 T_2))) \cos(f_0 X/V_0) \quad (2a)$$

$$M_y = B(1 - f_0 T_2 \exp(-X/(V_0 T_2))) \sin(f_0 X/V_0) \quad (2b)$$

where

$$A = \gamma f_0 M_0 B_1 T_2^2 / (1 + f_0^2 T_2^2) \quad (3a)$$

and

$$B = \gamma M_0 B_1 T_2 / (1 + f_0^2 T_2^2). \quad (3b)$$

Since it is assumed that there is no RF field beyond the excitor coil, the components of magnetisation of a given bolus of blood will undergo  $T_2$  decay, after leaving  $X_2$ , as follows

$$M'_x = M_x(X_2) \exp(-\Delta X/(V_0 T_2)) \quad (4)$$

$$M'_y = M_y(X_2) \exp(-\Delta X/(V_0 T_2)) \quad (5)$$

where  $\Delta X = X - X_2$ ,  $X > X_2$ .

The  $X$  (laboratory frame) component of magnetisation  $M_X$  (after the bolus has left the excitation region  $X_2$ ) is

$$M_X = M'_x \cos \omega t + M'_y \sin \omega t. \quad (6)$$

The NMR signal detected in the receiver coil of length  $L$  and separated from the excitor coil by  $\Delta l$  is

$$\text{EMF} = \beta \int_{X_3}^{X_4} \partial M_X / \partial t \, dX, \quad (7)$$

where  $X_3 = X_2 + \Delta l$ ,  $X_4 = X_3 + L$ , and  $\beta$  is the cross section of the blood vessel,  $\Delta l$  is the separation of the detector coil from the excitor coil end  $X_2$  (figure 1).

If the excitor frequency  $\omega/2\pi$  is set so that the bolus is exactly on resonance in the excitor coil region  $X_2 - X_1$ , then  $f_0 = 0$ . Then, using equations (2)-(6), equation (7) reduces to

$$\text{Signal EMF} = \omega \beta B \cos \omega t \int_{X_3}^{X_4} \exp(-(X - X_2)/(V_0 T_2)) \, dx \quad (8)$$

where

$$B = \gamma M_0 B_1 T_2; \quad X_4 - X_3 = L.$$

After carrying out the integration we arrive at

$$\text{Signal EMF} = B \omega T_2 Q_s \cos \omega t (\exp(-\Delta l/(V_0 T_2)) - \exp(-(\Delta l + L)/(V_0 T_2))) \quad (9)$$

where

$$Q_s = \beta V_0; \quad Q_s \text{ is the steady volume flow rate.}$$

A rigorous analysis shows that the right side of equations (8) and (9) should be multiplied by the factor  $(1 - \exp(-L_e/V_0 T_2))$ . If the excitor coil length  $L_e > 40$  cm, the flow signal is almost independent of the term arising out of excitor coil length within the human blood flow range  $0-50 \text{ cm s}^{-1}$ . Finally, when the signal  $I_{fs}$  is modulated and detected with reference to the same RF  $B_1$  (phase sensitive detection), the signal is expressed as

$$\text{Signal EMF } I_{fs}(V_0) = B\omega \cos \phi T_2 Q_s (\exp(-\Delta l/(V_0 T_2)) - \exp(-(L + \Delta l)/(V_0 T_2))). \quad (10)$$

Equation (10) may also be written as

$$\text{Signal EMF } I_{fs}(V_0) = C Q_s (\exp(-\Delta l/(V_0 T_2)) - \exp(-(L + \Delta l)/(V_0 T_2))). \quad (10a)$$

Here,  $C = B\omega T_2 \cos \phi$ , and  $\phi$  is the given phase introduced in the phase sensitive detection.

In the following computations, a  $T_2$  of 0.15 s, comparable to that of human blood is chosen. However, the results presented are qualitatively true for  $0.05 \text{ s} < T_2 < 0.5 \text{ s}$ .

Figure 2 shows the variation of the steady flow signal as a function of steady flow velocity for  $L = 10$  cm (lower set) and  $L = 50$  cm (top set). In each set,  $\Delta l$  for the top curve is 0 cm, increasing to 8 cm in the bottom curve. The figure shows that the signals due to steady blood flow depend sensitively on  $\Delta l$ ,  $L$ , and steady velocity  $V_0$  of blood. For a given velocity  $V_0$  and length  $L$ , the theoretical signal strength depends significantly on  $\Delta l$ . For a given change of  $\Delta l$ , the change of the signal strength is greater for longer detector coils. For large  $L (> 50 \text{ cm})$ , the signal varies almost linearly with  $L$  when  $\Delta l = 0$ . For  $\Delta l > 0$ , there is slight non-linearity when  $V_0$  is small. For small  $L$ , the variation is non-linear. For small velocities, the signals are independent of  $L$  for  $L$  greater than a certain value. For small  $L_e$ ,  $I_{fs}$  increases non-linearly up to a certain velocity, say  $V_s$ , where it begins to decrease for  $V_0 > V_s$ .  $V_s$  increases with  $L$  for fixed

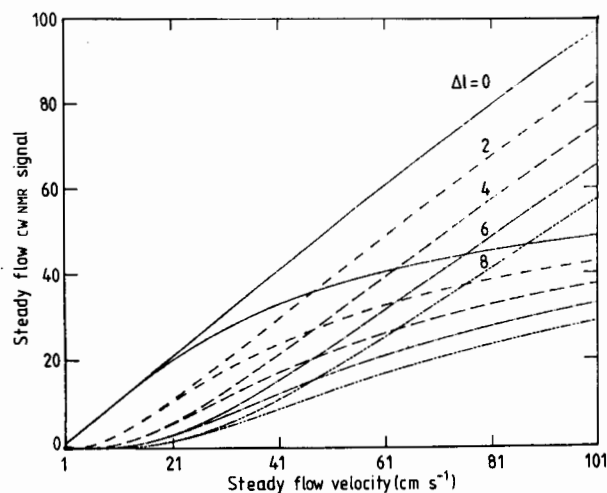


**Figure 2.** CW NMR steady flow signal strength,  $I_{fs}$  against steady velocity curves for two different lengths of the detector coil.  $L = 50$  cm for the upper set and  $L = 10$  cm for the lower set. In each set  $\Delta l$  varies from 0 to 8 cm for the top to bottom curve.

but small  $L_e$ . Therefore the CW NMR signal for a given velocity  $V_0$  depends on  $L$ ,  $L_e$ , and  $\Delta l$ .

## 2.2. Pulsatile flow

Blood flow in humans has both pulsatile and steady components, i.e.

$$V(t) = V_0 + V_{\text{pulse}}(t). \quad (11)$$

$V_{\text{pulse}}(t)$  is given by the following general equation (Halbach and Genthe 1988)

$$V_{\text{pulse}}(t) = (V_{\text{pulse}}^0/0.365) \exp(-4t) \sin(-1.5\pi t). \quad (12)$$

The denominator of 0.365 ensures that the peak occurs at  $V_{\text{pulse}}^0$ .  $V_{\text{pulse}}(t)$  may also be given (Battocletti 1986) by

$$V_{\text{pulse}}(t) = 23.092 V_{\text{pulse}}^0 (t/T)(1-t/T)^8. \quad (13)$$

The resultant time dependent CW NMR signal  $I_{\text{ps}}(t)$  is derived by substituting  $V(t)$  from equations (11) and (12) for  $V_0$  in equation (10) or (10a). This substitution is based on the assumption that the pulsatile flow change occurs over a time scale much longer than  $T_2$ . This condition is satisfied for human pulsatile blood flow ( $T_2 \approx 0.12$  s and an  $R$ - $R$  interval of 1 s). These theoretical predictions have been verified with measurements computed from exact analysis of the CW NMR signal for pulsatile flow. These analyses are the subject of another paper.

## 3.1. Estimation of steady blood flow (plug flow)

The theory predicts that, using the proper detection scheme, the static tissue signal as well as the direct coupling between the excitor coil and the detector coil can be minimised. In reality, however, the static tissue signal is comparable or even larger than the flow signal. Below we discuss a method to eliminate the static tissue signal from the detected flow signal and procedures to determine  $V_0$  accurately.

The observed signal,  $I_{\text{fs}}$ , is given by

$$I_{\text{fs}} = I_{\text{fs}}(V_0) + I_{\text{st}} \quad (14)$$

where  $I_{\text{fs}}(V_0)$  is given by equation (10) or (10a) and does not include static tissue signal. It should be noted that when pulsatile flow is present, the NMR flow signal is time dependent.  $I_{\text{fs}}$  in equation (14) would then correspond to the steady base line between periodic signals (figure 3).

Measuring the signal  $I0_{\text{fs}}$  for  $\Delta l = 0$  and  $I1_{\text{fs}}$  and  $I2_{\text{fs}}$  for two different but small values of  $\Delta l$ ,  $\Delta l_1 = 0.5$  cm, and  $\Delta l_2 = 1.0$  cm, from equation (9), we obtain

$$I0_{\text{fs}} = KV_0\beta c'(1 - \exp(-L/(V_0T_2))) + I_{\text{st}} \quad (15)$$

$$I1_{\text{fs}} = KV_0\beta c'(\exp(-\Delta l_1/(V_0T_2)) - \exp(-(\Delta l_1 + L)/(V_0T_2))) + I_{\text{st}} \quad (16)$$

$$I2_{\text{fs}} = KV_0\beta c'(\exp(-\Delta l_2/(V_0T_2)) - \exp(-(\Delta l_2 + L)/(V_0T_2))) + I_{\text{st}}. \quad (17)$$

The instrumental factor  $c'$  can be determined by calibrating the system with a fluid having  $T_2$  similar to that of blood.  $K = BT_2\omega$  should be known if  $B = \gamma B_1 T_2 M_0$  is known (i.e. one should know  $B_1$  and  $M_0$ , as well as  $T_2$ ). In the three expressions above for flow signal strengths, the static signal ' $I_{\text{st}}$ ' part received in the detector is assumed to remain essentially the same for values of  $\Delta l_1$  and  $\Delta l_2$  that are very small compared with large values of  $L$  (greater than 25 cm), as expected under the given

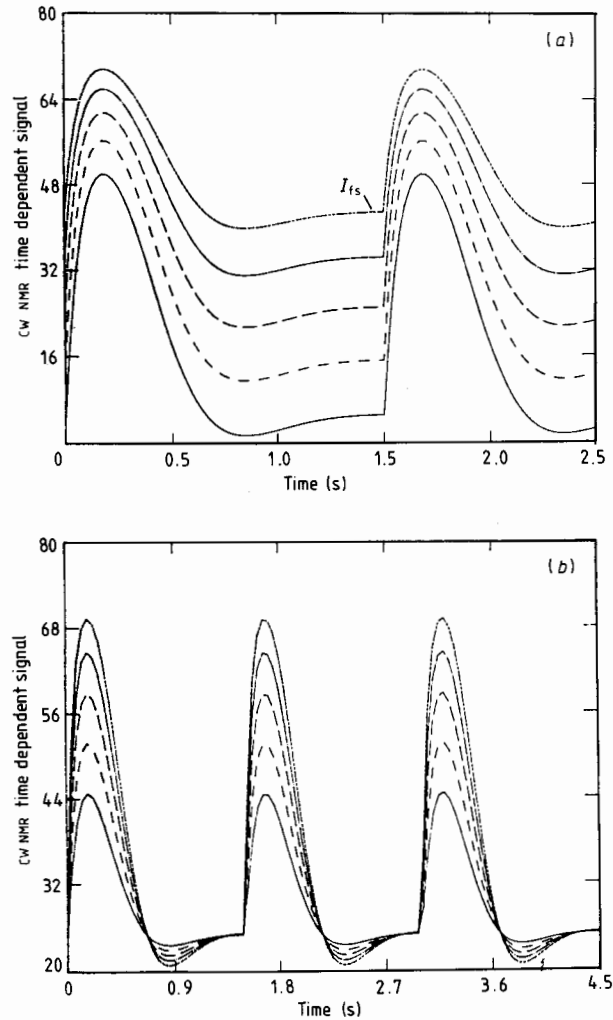


**Figure 3.** (a) Shows how NMR time dependent flow signal strength against  $V_0$  curves changes when  $V_0$  changes from  $5 \text{ cm s}^{-1}$  to  $45 \text{ cm s}^{-1}$  when  $V_{\text{pulse}} = 50 \text{ cm s}^{-1}$ . The peak to peak height decreases considerably with increases of  $V_0$ . (b) Computed CW NMR time dependent flow signal  $I_{ps}$  for  $L = 30$ ,  $L_c = 30 \text{ cm}$   $\Delta l = 0$  and  $V_{\text{pulse}}^0$  varies as a parameter from  $20 \text{ cm s}^{-1}$  for the lowermost curve to  $60 \text{ cm s}^{-1}$  for the uppermost curve.  $V_0 = 25 \text{ cm s}^{-1}$ . Time  $t = 0$  is counted from the moment the bolus enters the detector coil.

experimental arrangement (figure 1) and detection scheme as mentioned in the theory section.†

From equations (15)–(17), it is clear that the ratio,  $\xi$ , of the difference signals may be given by

$$\begin{aligned} \xi &= (I_{0fs} - I_{1fs}) / (I_{0fs} - I_{2fs}) \\ &= [1 - \exp(-\Delta l_1 / (V_0 T_2))] / [1 - \exp(-\Delta l_2 / (V_0 T_2))] \\ &= (\theta_1 - \theta_1^2 / V_0) / (\theta_2 - \theta_2^2 / V_0) \end{aligned} \quad (18)$$

† Even if this is not 100% true, the factor by which the  $I_{st}$  part will change would be a constant determined only by the given set-up and given  $\Delta l$ . This can be determined experimentally by using materials with  $T_2$  close to human tissue and introduced accordingly into equations (15)–(17).

where

$$\theta_1 = \Delta l_1 / T_2 \text{ and } \theta_2 = \Delta l_2 / T_2. \quad (19)$$

$\theta_1, \theta_2$  are determined if  $T_2$  is known.  $\xi$  can easily be calculated by experimentally obtaining the NMR flow signals, for three detector coil positions such as  $\Delta l = 0$ ,  $\Delta l = \Delta l_1 = 0.5$  cm, and  $\Delta l = \Delta l_2 = 1.0$  cm, with other experimental parameters remaining the same.  $V_0$  then can be estimated from equation (18), even if the cross section  $\beta$  of the blood vessel is not known. In the method described above one can determine the steady blood flow velocity  $V_0$  even without calibrating the system. However, calibration of the system with a known flow rate will allow determination of the total flow rate as well.

### 3.2. Estimation of total effective cross section of the blood vessels

From the difference of any two equations (15)–(17), we can determine the product  $K\beta$  of the system by substituting the value of  $V_0$  as determined above and using the values of  $L, T_2$ , and  $\Delta l$  which are known ( $K$  is known through  $B$  of equation (3b)). Then  $\beta$ , the total cross sectional area of the blood vessel with steady flow, can be determined. However, reliable results can also be obtained if the system is calibrated with a fluid of  $T_2$  similar to blood flowing at a known steady velocity through a tube of known cross sectional area. Then from the above equations one can determine 'K' of the CW system and the total cross section of the blood vessel. The total steady flow rate  $Q_s = \beta V_0$  can be estimated.

Because  $T_2$  for *in vivo* blood may vary from patient to patient and may therefore be an unknown quantity, determination of  $V_0$  using the above method would then require knowledge of either  $T_2$  or  $\beta$ . The latter may be determined quite reliably by magnetic resonance imaging of the blood vessel from which the CW NMR signals would be collected. The imaging for the determination of the blood vessel cross section and the CW NMR excitation for blood flow estimation should be performed separately, because the MRI technique would introduce significant magnetic field gradients that may invalidate the above theoretical considerations, if the  $B_0$  field inhomogeneity over the vessel cross section becomes greater than RF  $B_1$  field. However, they may be incorporated into the same system.

The quantity  $\alpha = V_0 T_2$  can be determined from

$$\xi = (\Delta l_1 / \alpha - \Delta l_1 / \alpha^2) / (\Delta l_2 / \alpha - \Delta l_2 / \alpha^2). \quad (20)$$

The quantity

$$C = K V_0 \beta c' = \gamma \omega \beta M_0 \alpha T_2 c' \quad (21)$$

is determined from the difference of any two equations (15)–(17) using the value of  $\alpha$  from equation (20). Then, using the value of  $\beta$  as determined from MRI, the *in vivo* blood  $T_2$  may be determined from equation (21).  $V_0$  can then be obtained from  $V_0 = \alpha / T_2$ . Otherwise (i.e. where the MRI facility for blood vessel imaging is not incorporated into the CW NMR system) the present CW NMR method can be applied for the determination of both  $V_0$  and  $\beta$  by using an average value of *in vivo* blood  $T_2$ , which is approximately 0.12 s. It appears that where both steady and pulsatile flows are present simultaneously, it is possible to determine  $T_2, V_0, \beta$  and the pulsatile flow



components using the present method only (i.e. without needing an MRI facility), as discussed in § 5.

#### 4. Estimation of pulsatile flow

##### 4.1. Effect of $V_0$ on the time dependent CW NMR signal due to $V_{\text{pulse}}(t)$

Figures 3–6 are computed for different  $V_0$  and  $V_{\text{pulse}}^0$ s assuming  $T_2 = 0.15$  s. The general results obtained are similar for  $T_2$  in the range  $0.075 \text{ s} < T_2 < 0.5$  s. Figure 3 shows the variation of the CW NMR net time dependent periodic signal strength for different values of  $V_0$  assuming  $\Delta l = 0$ .† As  $V_0$  increases, the time dependent part of the CW NMR signal decreases. The strength of the signal due to the steady flow,  $I_{\text{fs}}$ , also increases with  $V_0$ . This  $I_{\text{fs}}$  which is mixed with the static tissue signal as well, can be used as explained in §§ 3.1 and 3.2 to extract  $V_0$ ,  $\beta$ , etc. Figure 3(b) shows only the repeated periodic pulsatile flow signals when  $V_0$  is kept constant at  $25 \text{ cm s}^{-1}$  and  $V_{\text{pulse}}^0$  (denoted by VP1, etc) varies from 20 to  $60 \text{ cm s}^{-1}$ . The ratio of the corresponding peak height,  $I_{\text{pp}}$ , to  $V_{\text{pulse}}^0$  varies from 0.26 to 0.2, respectively. Figure 4 shows the peak-to-peak height of the time dependent part of the net CW NMR signal,  $I_{\text{pp}}$  for different values of steady velocities  $V_0$ ,  $\Delta l$ , and  $L$ . When  $L > 50$  cm and  $\Delta l = 0$ ,  $I_{\text{pp}}$  varies almost linearly with  $V_{\text{pulse}}^0$ , and the dependence of  $I_{\text{pp}}$  on  $V_0$  is not great. But when  $L$  is small, then for either  $\Delta l = 0$  or  $\Delta l > 0$ ,  $I_{\text{pp}}$  varies with  $V_{\text{pulse}}^0$  non-linearly and is significantly

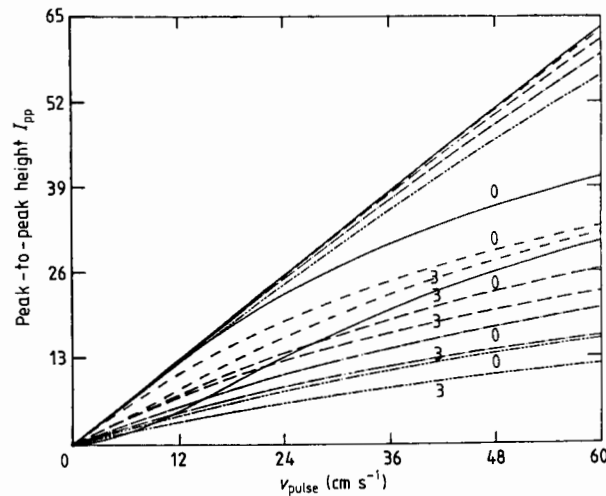


**Figure 4.** The peak to peak height  $I_{\text{pp}}$  against  $V_{\text{pulse}}^0$  curves. In each set,  $V_0 = 5 \text{ cm s}^{-1}$  for the continuous curve;  $V_0 = 15 \text{ cm s}^{-1}$  for the small dashed lines;  $V_0 = 25 \text{ cm s}^{-1}$  for the large dashed lines;  $V_0 = 35 \text{ cm s}^{-1}$  for the single dot dashed line;  $V_0 = 45 \text{ cm s}^{-1}$  for the double dots dashed lines.  $L = 50$  cm  $\Delta l = 0$  for the top set.  $L = 10$  cm for the lower sets in which  $\Delta l = 0$  and  $\Delta l = 3$  cm are marked. When  $L = > 50$  cm and  $\Delta l = 0$   $I_{\text{pp}}$  varies linearly with  $V_{\text{pulse}}^0$  and is less dependent on  $V_0$  than when  $L$  is small and  $\Delta l > 0$ .

† Time  $t = 0$  is counted from the moment the first bolus of fluid enters the detector coil. The signal is initially zero and then rises with time. In the case where time  $t = 0$  is the moment the blood bolus enters the excitor coil, the features are essentially the same except that there is no signal in the detector coil for a length of time  $\Delta t$  where

$$L_c = \int_0^{\Delta t} V(t) dt.$$

dependent on  $V_0$ . Figure 5 shows  $I_{pp}$  as a function of  $V_0$  when  $V_{pulse}^0$  is held constant at  $40 \text{ cm s}^{-1}$ . As  $L$  increases from the bottom to the top of the curve,  $I_{pp}$  decreases continuously with  $V_0$  for  $\Delta l = 0$ . For  $\Delta l > 0$ ,  $I_{pp}$  increases with  $V_0$  up to a certain velocity  $V_L$ , which increases with  $L$  (figure 6).  $I_{pp}$  decreases as  $V_0$  increases beyond  $V_L$ .

Let us define  $V_{pf}$  as the total flow per cardiac cycle. If the system with a large excitor coil ( $L_e > 40 \text{ cm}$ ) and a detector coil ( $L > 50 \text{ cm}$ ) is calibrated for one known  $V_{pulse}^0$ , i.e.  $I_{pp}$  is known (or the total integrated area for  $V_{pf}$ ), then the calibration could be used linearly for  $\Delta l = 0$  to estimate  $V_{pulse}^0$  (or  $V_{pf}$ ). For values of  $\Delta l > 0$ , the estimation would be expected to exhibit some error, which is a complicated function of  $L$ ,  $\Delta l$ ,  $V_{pulse}^0$ ,  $V_0$  and the point of calibration. Accurate estimation of  $V_0$  must be made

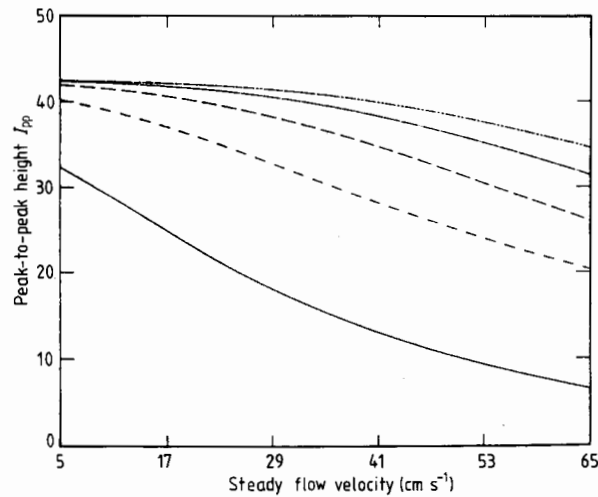


**Figure 5.**  $I_{pp}$  against  $V_0$  curves for fixed  $V_{pulse}^0$  ( $=40 \text{ cm s}^{-1}$ ) when the detector length  $L$  varies from  $10 \text{ cm}$  (bottom curve) to  $L = 50 \text{ cm}$  (top curve). It is seen that as  $L$  increases  $I_{pp}$  becomes less and less dependent on  $V_0$ .  $\Delta l = 0$ .

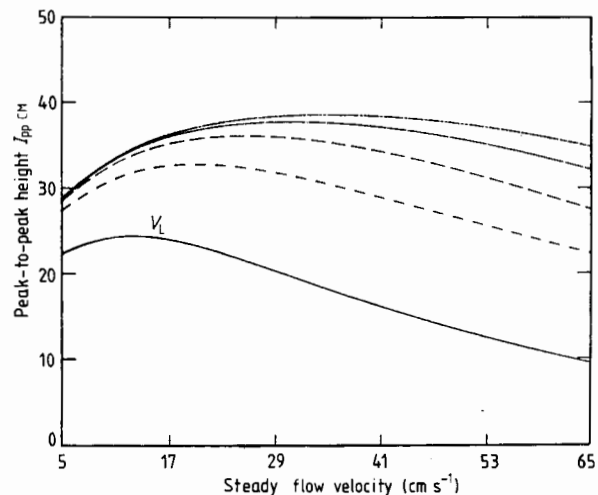


**Figure 6.** Same as figure 5 but with  $\Delta l = 3 \text{ cm}$ .  $I_{pp}$  tends to peak at a certain velocity  $V_L$  and then decrease beyond  $V_L$ .  $V_L$  increases with  $L$ .

in order to determine the true  $V_{\text{pulse}}^0$  in this case or for the case of small  $L$ , even with  $\Delta l = 0$ . It may be mentioned that  $I_{\text{fs}}$  is always independent of  $V_{\text{pulse}}^0$ .

#### 4.2. Estimation of true $V_{\text{pulse}}^0$

Beginning with equation (10a), as explained in § 2.2  $V_0$  is replaced by  $V(t)$  to compute  $I_{\text{ps}}(t)$ .

Thus

$$I_{\text{ps}}(t) = C_0 V(t) (\exp(-\Delta l / V(t) T_2) - \exp(-(\Delta l + L) / V(t) T_2)) \quad (22)$$

where

$$C_0 = K\beta c'. \quad V(t) \text{ is given by equations (11)-(13).}$$

We assume that the length of the excitor coil is greater than 40 cm so that the expression  $[1 - \exp(-L_e / VT_2)]$  is close to unity within the range of human blood flow. The measured base to peak height  $I_{\text{pb}}^m$  or the peak to peak height  $I_{\text{pp}}^m$  of the pulsatile flow signal may be expressed as

$$I_{\text{pb}}^m(\Delta l) = C_0 [V_1 \{ \exp(-\Delta l / (T_2 V_1)) - \exp(-(\Delta l + L) / (V_1 T_2)) \} - V_0 \{ \exp(-\Delta l / (T_2 V_0)) - \exp(-(\Delta l + L) / (V_0 T_2)) \}] \quad (23)$$

$$I_{\text{pp}}^m(\Delta l) = C_0 [V_1 \{ \exp(-\Delta l / (T_2 V_1)) - \exp(-(\Delta l + L) / (V_1 T_2)) \} - V_2 \{ \exp(-\Delta l / (T_2 V_2)) - \exp(-(\Delta l + L) / (V_2 T_2)) \}] \quad (24)$$

where

$$V_1 = V_0 + V_{\text{pulse}}^0 \quad (25)$$

and

$$V_2 = V_0 - 0.0695 V_{\text{pulse}}^0 \quad (26)$$

when  $V_{\text{pulse}}(t)$  is given by equation (12). For  $V_{\text{pulse}}(t)$  as given by equation (13),  $V_2$  is given by  $V = V_0$ .  $C_0 = K\beta c'$ . The instrumental factor  $c'$  can be determined by calibration using the same  $B_1$ ,  $B_0$ ,  $L$ , and  $L_e$  as for the unknown signals.

It should be noted that  $I_{\text{pp}}^m$ ,  $I_{\text{pb}}^m$  is not influenced by the static tissue signal because it is the difference between the maximum and the minimum points of the time dependent pulsatile flow signal, or the signal above the base line. Similarly,  $I_{\text{ps}}(t)$  when measured from the base line is also independent of the static tissue signal. We can determine  $I_{\text{pp}}^m(\Delta l)$  for values  $\Delta l_1$ ,  $\Delta l_2$ . Then we can determine the ratio of  $r(\Delta l_1, \Delta l_2) = I_{\text{pp}}^m(\Delta l_1) / I_{\text{pp}}^m(\Delta l_2)$ , and obtain  $V_{\text{pulse}}^0$  using the value of  $V_0$  as determined by the method of § 3 and equations (25)-(26), and the average value of  $T_2$  for human blood. However,  $V_{\text{pulse}}^0$  and  $V_0$  can also be obtained independently from two values of  $r$  (for different values of  $\Delta l_1$  and  $\Delta l_2$ ) and using equations (25) and (26).

From the discussion above, it may be possible also to determine all the quantities such as  $V_0$ ,  $V_{\text{pulse}}^0$ ,  $\beta$ , and  $T_2$  independently for a particular patient without recourse to any other technique such as magnetic resonance imaging or use of an average value of  $T_2$ . For example, the quantities  $V_1 T_2$  and  $V_2 T_2$  can be determined from different ratios  $r(\Delta l_1, \Delta l_2)$  using equations (23) and (24). Then using the value of  $\infty = V_0 T_2$  as determined in § 3 and equations (25) and (26), we can determine  $V_0$ ,  $V_{\text{pulse}}^0$ , and  $T_2$  uniquely. Then  $\beta$  can be determined as discussed in § 3.2.

## 5. Conclusion

It is shown that using the method of 'CW NMR excitation with a separate detection system' as discussed above, one can virtually eliminate the problem of static tissue signal and quantitatively estimate both the pulsatile and steady components of blood flow velocity and rates. Furthermore, the measurement of pulsatile component of the flow velocity or rate only from the pulsatile part of the time dependent CW NMR signal would be erroneous without correction for steady flow velocity  $V_0$ . This fact is primarily though not completely due to the exponential  $T_2$  decay of the blood magnetisation, which depends non-linearly on blood flow velocity, whether steady or pulsatile. However, to measure the steady flow rate  $Q_s$ , signals must be obtained for three small values of  $\Delta l$ . Then the static tissue signal ' $I_{st}$ ' can be eliminated and both the steady flow velocity  $V_0$  and the flow rate  $Q_s = \beta V_0$  ( $\beta$  = total cross section area of the blood vessels) can be obtained, as well as the pulsatile flow  $V_{pulse}^0$ . The time dependent CW NMR signals are linearly dependent on pulsatile velocity only when a large detector coil ( $L_e > 40$  cm,  $T_2 = 0.15$  s and  $L > 50$  cm for  $T_2 = 0.3$  s) is used with  $\Delta l = 0$ . With small excitor and detector coils it is also possible by the present method to determine independently and uniquely  $T_2$ ,  $V_0$ ,  $V_{pulse}^0$ , and  $\beta$  when both steady and periodic pulsatile flows are simultaneously present. For a small excitor coil, the same procedure as discussed in § 4.2 applies, except a factor  $(1 - \exp(-L_e/VT_2))$  must be multiplied on the right hand side of equations (22)-(24).

## Appendix 1. Parabolic flow

So far we have considered plug or uniform flow of blood through the vessel of uniform cross section  $\beta$ . For non-plug flow of blood, when the flow velocity is parabolic across the vessel cross section, the NMR blood flow signal expression may be obtained by integrating equation (10a) over the cross section of the blood vessel

$$I_{fs} = C 2\pi \int_0^R V(r) (\exp(-\Delta l/V(r)T_2) - \exp(-(\Delta l + L)/V(r)T_2)) r dr \quad (A1)$$

where  $R$  is the radius of the vessel. The parabolic flow velocity  $V$  is given by

$$V(r) = V_c(1 - r^2/R^2) \quad (A2)$$

$\pi R^2 = \beta$  the cross section of the blood flow vessel.

It can be easily shown that the total flow rate  $Q_s$  for a parabolic flow with peak velocity of  $V_c$  is the same as that with steady uniform velocity:  $V_0 = V_c/2$ . With this consideration, we compare the NMR signals against  $V_0$  curves due to the parabolic flow profile (with peak velocity  $V_c = 2V_0$ , the total flow rates in both cases are then the same) with that of uniform or plug flow signal curves in figures 7 and 8. In both figures 7 and 8,  $\Delta l$  increases from 0 (top pair of curves) to 8 (bottom pair of curves) in steps of 2 cm.  $T_2 = 0.175$ s. In figure 7 (for small  $L = 10$  cm, where  $\Delta l = 0$ ), the parabolic flow signal is smaller than the uniform flow signal. For a given  $\Delta l$  and  $\Delta l \gg 0$ , the two curves cross each other at a certain steady flow velocity  $V_0 = V_{pr}$ . The parabolic flow signal is larger than the uniform flow signal for  $V_0 > V_{pr}$ .  $V_{pr}$  increases with  $\Delta l$  for small  $L$ . The situation is different for  $L = 50$  cm or a large detector coil. The parabolic flow signals are always larger than the uniform flow signal (figure 8) except for  $\Delta l = 0$  when both the parabolic flow signal and the uniform flow signals are the same and vary linearly with  $V_0$  as discussed earlier. Some non-linearity in the flow signals is always present for  $\Delta l \gg 0$ . It should be noted that one cannot distinguish

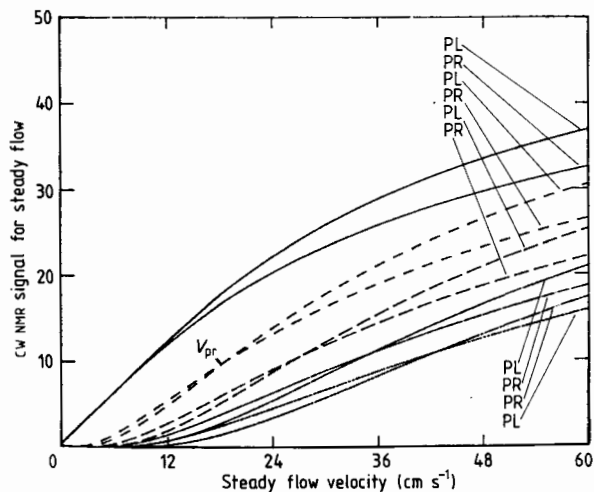


**Figure 7.** CW NMR signal for steady flow against steady velocity curves for plug flow (marked PL) and parabolic flow (marked PR) for  $L = 10$  cm and different values of  $\Delta l$ . The plug flow curve crosses the parabolic curve at  $V_{pr}$ . In general the plug flow signal is larger than the parabolic flow signal when  $L$  is small.

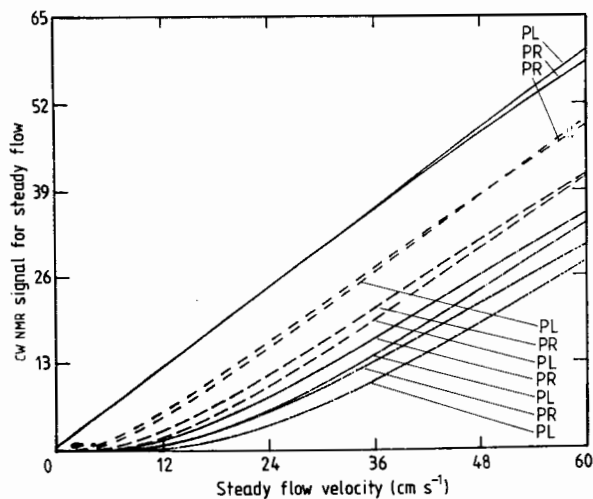


**Figure 8.** Same as figure 7 but with  $L = 50$  cm. The parabolic flow is in general larger than the plug flow except when  $\Delta l = 0$ .

between the two different flow profiles, parabolic or uniform plug flow, from the measurement of the CW NMR signals. By applying techniques similar to slice selection in MRI, one should be able to obtain the parabolic flow distributions. All the essential features as discussed for plug flow hold good for parabolic flow as well.

### Acknowledgments

The author acknowledges and appreciates discussions with Professor P R Moran, Professor E Hiltbrand, Professor W Sobol, and Mr W Hinson. The author thanks Donna Garrison and Joyce Hill for their assistance in the preparation of the manuscript. This research was supported by NIH grant number CA 09487-05.

## Résumé

Etude théorique de l'estimation du flux sanguin stationnaire et pulsé et de la section des vaisseaux sanguins par excitation RMN CW.

Dans cet article, l'auteur montre, sur le plan théorique, que quand un embol de sang magnétisé pénètre à la résonance dans une bobine d'excitation RMN à émission continue (CW) de longueur  $L_e$  et que le signal de la magnétisation transverse, précédant et décroissant selon  $T_2$ , des spins du sang circulant est par la suite détecté par une bobine de détection de longueur  $L$  séparée de la bobine d'excitation par une distance  $\Delta l$ , alors l'enregistrement des signaux RMN CW en trois positions telles que  $\Delta l = 0, 0,5$  et  $1,0$  cm permet d'éliminer le signal dû aux tissus statiques et de mesurer exactement la composante stationnaire  $V_0$  ainsi que la section  $\beta$  du vaisseau. La partie liée au temps du signal RMN CW, qui dépend de l'impulsion  $V(t)$ , est aussi dépendante de  $V_0$ , de manière non linéaire, à moins que  $L$  et  $L_e$  soient toutes les deux supérieures à 50 cm, et  $\Delta l$  égal à zéro. Enfin, les méthodes permettant d'obtenir de vraies impulsions  $V(t)$  à partir du signal RMN CW, après application de corrections convenables du flux stationnaire, font l'objet d'une discussion.

## Zusammenfassung

Theoretische Untersuchungen zur Bestimmung des kontinuierlichen und des pulsierenden Blutflusses und der Blutgefäßquerschnitte mit Hilfe der CW NMR-Anregung.

In der vorliegenden Arbeit wird theoretisch gezeigt, daß bei Eintritt eines magnetisierten Blutbolus in eine CW NMR-Magnetspule der Länge  $L_e$  bei Resonanz und Abfall des  $T_2$ -Signals, die statischen Gewebesignale eliminiert und sowohl die kontinuierliche Komponente  $V_0$  als auch der totale Gefäß-querschnitt  $\beta$  genau gemessen werden kann durch Aufnahme der CW NMR-Signale bei drei Positionen, wie z.B.  $\Delta l = 0, 0,5$  und  $1,0$  cm, wenn die transverse Magnetisierung der Spins des fließenden Blutes mit einer Detektorspule der Länge  $L$ , die von der Magnetspule durch einen Abstand  $\Delta l$  getrennt ist, nachgewiesen werden kann. Der zeitabhängige Teil des CW NMR-Signals, der von  $V_{\text{puls}}(t)$  abhängt, ist auch nicht-linear von  $V_0$  abhängig, außer, wenn sowohl  $L$  wie auch  $L_e$  größer als 50 cm sind und  $\Delta l$  Null ist. Abschließend werden Methoden zur Bestimmung echter  $V_{\text{puls}}(t)$ -Werte aus dem CW NMR-Signal nach Anwendung geeigneter Korrekturen des kontinuierlichen Flusses diskutiert.

## References

- Axel L 1984 Blood flow effects in magnetic resonance imaging *Am. J. Rontegenol.* **143** 1157-66
- Axel L, Shimakawa A and MacFall J 1986 A time-of-flight method of measuring flow velocity by magnetic resonance imaging *Magn. Reson. Imaging* **4** 199-205
- Battocletti J H 1986 Blood flow measurement by MRI *Rev. Biomed. Eng.* **13** 311-67
- Battocletti J H, Halbach R E, Salles-Cunha S X and Sances A Jr 1981 The NMR blood flowmeter—theory and history *Med. Phys.* **8** 435-43
- Battocletti J H, Halbach R E, Sances A Jr, Larson S J, Bowman R L and Kudravcev V 1979 Flat crossed-coil detector for blood flow measurement using nuclear magnetic resonance *Med. Biol. Eng. Comput.* **17** 183-91
- Caro C G, Pedley T J, Schroter R C and Seed W A 1978 *The Mechanics of Circulation* (Oxford: Oxford University Press)
- Devine R A B, Clarke L P, Vaughan S and Serafini A 1982 Theoretical analysis of the two-coil method for measuring fluid flow using nuclear magnetic resonance *Med. Phys.* **9** 668-72
- Halbach R E, Battocletti J H, Sance A Jr, Bowman R L and Kudravcev V 1980 Ranging for individual artery flow in the nuclear magnetic resonance flow meter *IEEE Trans. Biomed. Eng.* **27** 546 (abstr.)
- Halbach R E and Genthe W 1988 Private communication
- Hayward R J, Packer K J and Tomlinson D J 1972 Pulsed field-gradient spin echo NMR studies of flow in fluids *Mol. Phys.* **23** 1083-102
- Heminaga M A, deJager P A and Sonneveld A 1977 The study of flow by pulsed nuclear magnetic resonance. I. Measurement of a stationary phase using a difference method *J. Magn. Reson.* **27** 359-70
- Moran P R 1982 A flow velocity zuematographic interlace for NMR imaging in humans *Magn. Reson. Imaging* **1** 197-203

- Moran P R *et al* 1987 NMR velocity selective excitation composites for flow and motion imaging and suppression of static tissue signal *IEEE Trans. Med. Imaging* **MI-6(2)** 141-7
- O'Donnell M 1985 NMR blood flow imaging using multiecho, phase contrast sequences *Med. Phys.* **12** 59-64
- Redpath T W, Norris D G, Jones R A and Hutchison J M S 1984 A new method of NMR flow imaging *Phys. Med. Biol.* **29** 891-5
- Salles-Cunha S X, Halbach R E, Battocletti J H and Sances A Jr 1981 The NMR blood flowmeter—applications *Med. Phys.* **8** 452-8
- Salles-Cunha S X, Halbach R E, Battocletti J H, Sances A Jr and Evans S M 1982 *In vivo* evaluation of nuclear magnetic resonance flowmetry: blood flow through the normal forearm *Med. Instrum.* **16** 295-8
- Saloner D, Hinson W H, Moran P R and Tsui B M W 1988 MR flow imaging in projection through a stationary surround *J. Comput. Assist. Tomog.* **12** 122-9
- Saloner D, Moran P R and Tsui B M W 1987 Quantitative velocity determination in MRI of flow using a measure independent of the absolute intensity *Magn. Reson. Imaging* **5(S1)** 37 (abstr.)
- Singer J R 1959 Blood flow rates by nuclear magnetic resonance measurements *Science* **130** 1652-3
- Singer J R and Grover T 1972 *Modern Developments in Flow Measurements: Proc. Int. Conf., Harwell, 21-23 September 1971* ed. C G Clayton (London: Peregrinus)
- Slichter C P 1963 *Principles of Magnetic Resonance* ed. F Seitz (New York: Harper and Row) p 30
- Stejskal E O and Tanner J E 1965 Spin diffusion measurement: spin echoes in the presence of a time dependent gradient *J. Chem. Phys.* **42** 288-92
- Van Dijk P J 1984 Direct cardiac NMR imaging of heart wall and blood flow velocity *J. Comput. Assist. Tomog.* **8** 429-36.